17th World Conference on Earthquake Engineering, 17WCEE
Sendai, Japan - September 13th to 18th 2020

EFFECT OF AN ADJACENT WALL ON THE OVERTURNING OF A SLIDING-ROCKING BLOCK SUBJECTED TO PULSE EXCITATION

Y.Bao[(1)], D. Konstantinidis[(2)]

[(1)] *Lecturer, School of Civil Engineering and Architecture, Wuhan University of Technology, bao.yu@whut.edu.cn*
[(2)] *Assistant Professor, Department of Civil and Environmental Engineering, University of California Berkeley, konstantinidis@berkeley.edu*

Abstract

A rigid block placing next to a rigid boundary can be found in many applications of non-structural components in buildings, a typical example is a bookcase and partition wall system. Understanding the dynamics of such a system can help stakeholders better quantify the seismic risk and associated economic losses during an earthquake event. To this end, this paper first describes the governing equations of motion for different response modes of the block, which includes pure sliding, pure rocking and combined sliding-rocking motion. Subsequently, a novel approach based on classical principle of impulse and momentum is developed to handle the rigid block impacting the adjacent wall. The accuracy of the developed model is verified by comparing time-history response with a general-purpose rigid body model in which contact and impact are modeled using a viscoelastic force model. Since the developed model has significant improvement in terms of computational efficiency, it is used for further investigation in this study. The effects of the adjacent wall on the overturning of the rigid block are explored with analytical antisymmetric Ricker pulses. The influence of different parameters is evaluated by comparing the shapes of overturning spectra of the unobstructed and obstructed blocks. It is found that the existence of the adjacent wall significantly complicates the trends of toppling of the block. Generally, decreasing the friction coefficient of the ground, decreasing the clear wall distance and coefficient of restitution of the wall can enhance the stability of the block.

Keywords: unilateral constraint; sliding; rocking; impact; overturning.

1. Introduction

A freestanding planar rigid block subjected to base excitation has been received significant attention from the earthquake engineering community since the seminal work published by Housner [1]. The considerable interest in this problem may be attributed to the fact that many non-structural components can be idealized as a rigid block resting on a surface. Depending on the aspect ratio of the block, the frictional resistance and excitation amplitude, the planar block can exhibit five different modes: (1) rest; (2) pure sliding; (3) pure rocking; (4) combined sliding-rocking; and (5) free-flight. Criteria to initiate these modes are already given in [2]. In the past decades, many studies have been devoted to better understanding of seismic risks of non-structural components whose responses are dominated by pure sliding motion (e.g. [3], [4]) or pure rocking motion (e.g. [5], [6], [7]). A few notable studies have focused on the dynamics of sliding-rocking block. The first study, which developed governing equations of motion for a sliding-rocking block, is reported in [8]. Subsequently, Ishiyama [9] and Taniguchi [10] separately investigated the complicated response of a rigid block considering different modes during base excitation. Shenton et al. [11] presented a general framework to model the important impact phenomenon that may occur during base excitation. Compared to [9], Shenton's work [11] eliminates a priori knowledge of tangent coefficient of restitution, which seems impossible to determine from experiments.

Almost all the previously mentioned studies assumed that the planar block does not interact with adjacent boundaries during its motion. This assumption is often unrealistic. For example, bookcases in real buildings are nearly always placed next to a wall, and the presence of an adjacent wall can significantly affect the response of a bookcase, as demonstrated in [12]. Therefore, to better understand the responses of such a system under base excitation and help stakeholders quantify the associated seismic risks, this paper investigates the dynamics of a sliding-rocking block with a rigid boundary in its vicinity. First, the equations of motion governing each response mode, as well as the commencing conditions, are presented. Then a novel approach based on principle of impulse and momentum is developed to handle the block impacting with an adjacent boundary. The accuracy of the proposed model is verified by comparing its time history response with a general-purpose rigid body model in which impact and contact are modeled with a viscoelastic force model. Since the developed model has significant improvement in terms of computational efficiency, it is used for further investigation in this study. The effects of the adjacent wall on the overturning of the rigid

block are explored with analytical antisymmetric Ricker pulses ([13], [14]). The influence of different parameters is evaluated by comparing the shapes of overturning spectra of the unobstructed and obstructed blocks. It is found that the existence of the adjacent wall significantly complicates the trends of toppling of the block. Generally, decreasing the friction coefficient of the ground, decreasing the clear wall distance and coefficient of restitution of the wall can enhance the stability of the block.

2. Problem definition and equations of motion

2.1 Problem definition

The problem is schematically shown in Fig. 1. The freestanding block has a width of 2B and a height of 2H, or equivalently with a radius of R ($R = \sqrt{B^2 + H^2}$) and an angle of α ($\alpha = atan(B/H)$). There is a rigid wall placed adjacent to the left side of the block. The distance between the centroid of the block to the wall is δ_l. The block has three degrees-of-freedom, two horizontal translational DOFs and one rotational DOF, as depicted in Fig. 1. During base excitation, the resultant forces between the block and the ground are denoted as f_x and f_y. The finite friction coefficient on the ground is denoted as μ, while the wall is assumed frictionless. Since we are more interested in the rocking behavior of the block, it may exhibit four modes during earthquake excitation: rest, pure rocking, combined sliding-rocking and free-flight. In this study, the free-flight mode is excluded, which is also adopted by previous studies ([6] ,[7]) on the rocking problem.

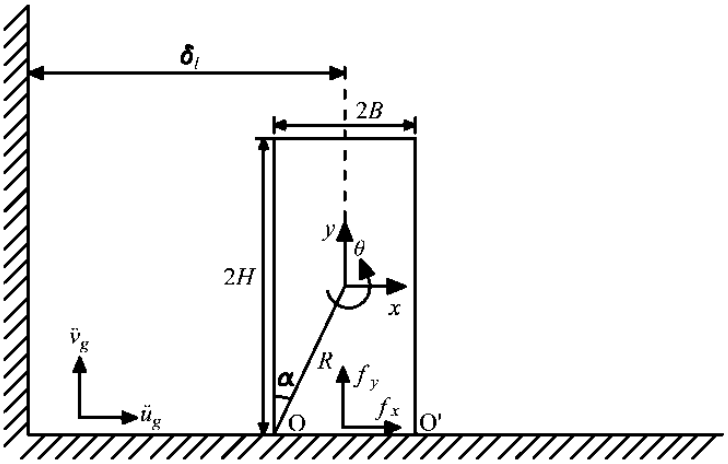

Fig. 1 Schematic drawing of a freestanding block placed adjacent to a left side wall

2.2 Equations of motion

For the block to exhibit rocking motion first from the rest mode, the following condition must be satisfied:

$$\mu_s \geq \tan\alpha \tag{1}$$

The commencing condition for pure rocking motion is:

$$\left|\ddot{u}_g\right| \geq \tan\alpha\left(\ddot{v}_g + g\right) \tag{2}$$

And the governing equation of motion for pure rocking motion is:

$$\frac{4}{3}R\ddot{\theta} = \ddot{u}_g\cos(\alpha - |\theta|) - S_\theta\sin(\alpha - |\theta|)\left(\ddot{v}_g + g\right) \tag{3}$$

where $S_\theta = S(\theta)$.

During pure rocking motion, the horizontal and vertical acceleration at the centroid of block can be expressed:

$$\ddot{x} = -S_\theta R\sin(\alpha - |\theta|)\dot{\theta}^2 - R\cos(\alpha - |\theta|)\ddot{\theta} \tag{4}$$

$$\ddot{y} = -R\sin(\alpha - |\theta|)\dot{\theta}^2 + S_\theta R\cos(\alpha - |\theta|)\ddot{\theta} \tag{5}$$

Therefore the rocking motion will be sustained provided the condition $|f_x| \leq \mu_s|f_y|$ is satisfied, or:

$$\left|\ddot{x} + \ddot{u}_g\right| \leq \mu_s\left|\ddot{y} + g + \ddot{v}_g\right| \tag{6}$$

If Eq. (6) is violated, the block will switch from pure rocking mode to combined sliding-rocking mode with the following equation of motion:

$$\ddot{\theta} + 4p^2 \frac{S_\theta[\sin(\alpha-|\theta|)+\eta\cos(\alpha-|\theta|)]\left[1+\frac{\ddot{v}_g}{g}-3\cos(\alpha-|\theta|)\dot{\theta}_p^2\right]}{1+3\sin^2(\alpha-|\theta|)+3\eta\sin(\alpha-|\theta|)\cos(\alpha-|\theta|)} = 0 \quad (7)$$

$$\ddot{x} + 4p^2 R \frac{\frac{\eta S_\theta}{3}\left[1+\frac{\ddot{v}_g}{g}-3\cos(\alpha-|\theta|)\dot{\theta}_p^2\right]}{1+3\sin^2(\alpha-|\theta|)+3\eta\sin(\alpha-|\theta|)\cos(\alpha-|\theta|)} = -\ddot{u}_g \quad (8)$$

where $p = \sqrt{3g/(4R)}$, $\eta = \mu_k S_\theta S_{\dot{x}_o}$, $\dot{\theta}_p = \dot{\theta}/(2p)$, $S_{\dot{x}_o} = S(\dot{x}_o)$, and $\dot{x}_o = \dot{x} + R\cos(\alpha - |\theta|)\dot{\theta}$.

The presence of the signum function (i.e. $S_{\dot{x}_o}$) makes the numerical evaluation of the equations of motion very difficult. To overcome this difficulty, it is proposed in [15] replacing $S_{\dot{x}_o}$ with an ordinary differential equation:

$$\dot{z} = \frac{1}{u_y}[-\gamma|\dot{x}_o|z|z|^{n-1} - \beta\dot{x}_o|z|^n + \dot{x}_o] \quad (9)$$

in which uy is the yield displacement, n is the exponent number, and β and γ are parameters controlling the shape of hysteresis loop. In this study, unless otherwise stated, the following values are used for these parameters: $u_y = 1.0 \times 10^{-5}$m, $\beta = \gamma = 0.5$, $n = 2$.

The equations of motion for rocking and combined sliding-rocking are not continuous when the rotation angle becomes zero, which indicates impact with ground happens. In this study the approach proposed in [11] is adopted to handle the impact of block with the ground, which relates the postimpact velocities of the block with the preimpact ones using classical impulse and momentum principle.

3. Approach to handle impact of block with an adjacent wall

This section presents a novel approach to handle the impact of block with an adjacent wall. The approach assumes that the duration of impact with wall is very short so the position of the block does not change while its velocity changes instantaneously. Classical impulse and momentum theory is used to determine the postimpact velocities of the block. Meanwhile, the preimpact and postimpact velocities normal to the impact point *i* is related through the classical coefficient of restitution of the wall e_w. The key point in this approach is to uniquely determine the postimpact velocities without violating any physical constraint of this problem. In this section, the preimpact velocities are denoted with subscript 1, while the postimpact ones are denoted with subscript 2. As noted, free-flight mode is excluded in this approach. There are three possible scenarios in which block impacts with the adjacent wall, as shown in Fig. 2. This section focuses on scenario (I), for a more detailed description of this approach, refer to [16].

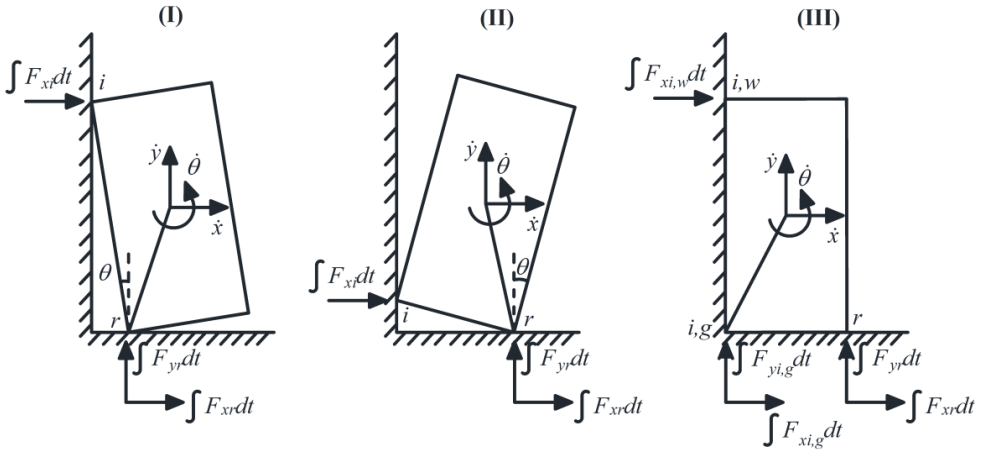

Fig. 2 (I) top corner impacting adjacent wall; (II) bottom corner impacting adjacent wall; (III) both corners impacting adjacent wall simultaneously

The condition for top corner impacting with a left side wall is given by:

$$x - R\sin(\alpha + \theta) = -\delta_l \quad (10)$$

The two orthogonal components of the velocities at the impact corner *i* and rotation corner *r* before and after the impact can be written as:

$$\dot{x}_{i1} = \dot{x}_1 - R\cos(\alpha + |\theta|)\dot{\theta}_1;\ \dot{y}_{i1} = \dot{y}_1 - S_\theta R\sin(\alpha + |\theta|)\dot{\theta}_1 \quad (11)$$

$$\dot{x}_{r1} = \dot{x}_1 + R\cos(\alpha - |\theta|)\dot{\theta}_1\ ;\ \dot{y}_{r1} = \dot{y}_1 - S_\theta R\sin(\alpha - |\theta|)\dot{\theta}_1 \quad (12)$$

$$\dot{x}_{i2} = \dot{x}_2 - R\cos(\alpha + |\theta|)\dot{\theta}_2\ ;\ \dot{y}_{i2} = \dot{y}_2 - S_\theta R\sin(\alpha + |\theta|)\dot{\theta}_2 \quad (13)$$

$$\dot{x}_{r2} = \dot{x}_2 + R\cos(\alpha - |\theta|)\dot{\theta}_2;\ \dot{y}_{r2} = \dot{y}_2 - S_\theta R\sin(\alpha - |\theta|)\dot{\theta}_2 \quad (14)$$

and the principle of linear and angular impulse and momentum requires that:

$$m\dot{x}_1 + \int F_{xi}dt + \int F_{xr}dt = m\dot{x}_2 \quad (15)$$

$$m\dot{y}_1 + \int F_{yr}dt = m\dot{y}_2 \quad (16)$$

$$I\dot{\theta}_1 + \int F_{xr}dt\, R\cos(\alpha - |\theta|) - S_\theta \int F_{yr}dt\, R\sin(\alpha - |\theta|) - \int F_{xi}dt\, R\cos(\alpha + |\theta|) = I\dot{\theta}_2 \quad (17)$$

Substituting Eq. (15) and (16) into (17) yields:

$$I\dot{\theta}_1 - mRS_\theta\sin(\alpha - |\theta|)(\dot{y}_2 - \dot{y}_1) - mR\cos(\alpha + |\theta|)(\dot{x}_2 - \dot{x}_1) + R[\cos(\alpha + |\theta|) + \cos(\alpha - |\theta|)]\int F_{xr}dt = I\dot{\theta}_2 \quad (18)$$

Eq. (18) has four unknowns: $\dot{x}_2$, $\dot{y}_2$, $\dot{\theta}_2$ and $\int F_{xr}dt$; therefore, three additional conditions are required to get a unique solution for the postimpact velocities. The first condition is using the coefficient of restitution between the block and the wall: $\dot{x}_{i2} = -e_w\dot{x}_{i1}$. With Eq. (11) and (13), the following equation is obtained(13)(13)(13)(13):

$$\dot{x}_2 = e_w R\cos(\alpha + |\theta|)\dot{\theta}_1 + R\cos(\alpha + |\theta|)\dot{\theta}_2 - e_w\dot{x}_1 \quad (19)$$

The second condition comes from the no-free-flight assumption. Consequently, the postimpact vertical velocity at the rotation corner must be zero, $\dot{y}_{r2} = 0$, as any value greater than zero will result in detachment from the ground and value less than zero is not physically meaningful. Thus Eq. (14) gives:

$$\dot{y}_2 = S_\theta R\sin(\alpha - |\theta|)\dot{\theta}_2 \quad (20)$$

Three additional physical constraints for this problem are:

(1) The impulse at the impact corner must not be less than zero for Case (I). This constraint may be expressed as $S_\theta \int F_{xi}dt \geq 0$, and with Eq. (15) we can have:

$$S_\theta \int F_{xr}dt \leq mS_\theta(\dot{x}_2 - \dot{x}_1) \quad (21)$$

(2) The postimpact horizontal velocity at the impact corner cannot result in penetration into the wall, this constraint can be expressed as:

$$S_\theta\dot{x}_{i2} = S_\theta\dot{x}_2 - S_\theta R\cos(\alpha + |\theta|)\dot{\theta}_2 \geq 0 \quad (22)$$

(3) There is no net increase in the kinetic energy during impact.

These constraints cannot provide a unique solution to this problem, and it is first assumed there is sufficient friction so sliding does not occur at the rotation corner during impact, then it is verified by examining the following condition:

$$\left|\int F_{xr}dt\right| \leq \mu_s\left|\int F_{yr}dt\right| \quad (23)$$

If Eq. (23) is violated, then friction is insufficient to prevent sliding. In either case, the postimpact velocities can then be uniquely determined. The subsequent discussion is divided into these two mutually exclusive cases.

There is sufficient friction to prevent sliding during impact

Since there is sufficient friction to prevent sliding during impact, the postimpact horizontal velocity at the rotation corner is zero, i.e. $\dot{x}_{r2} = 0$, which gives:

$$\dot{x}_2 = -R\cos(\alpha - |\theta|)\dot{\theta}_2 \quad (24)$$

Combining Eq. (19) and (24), the postimpact velocities can be written as:

$$\dot{\theta}_2 = \frac{e_w\frac{\dot{x}_1}{\dot{\theta}_1} - e_w R\cos(\alpha+|\theta|)}{R[\cos(\alpha+|\theta|)+\cos(\alpha-|\theta|)]}\dot{\theta}_1 = \xi\dot{\theta}_1;\ \dot{x}_2 = -R\cos(\alpha - |\theta|)\xi\dot{\theta}_1;\ \dot{y}_2 = S_\theta R\sin(\alpha - |\theta|)\xi\dot{\theta}_1 \quad (25)$$

Since Eq. (19) is used, Eq. (22) is automatically satisfied. With all the postimpact velocities available, substituting them into Eq. (18) the impulse at the rotation corner $\int F_{xr}dt$ can be evaluated as:

$$\int F_{xr}dt = \frac{mRS_\theta\sin(\alpha-|\theta|)[S_\theta\xi R\sin(\alpha-|\theta|)\dot{\theta}_1 - \dot{y}_1] - mR\cos(\alpha+|\theta|)[\xi R\cos(\alpha-|\theta|)\dot{\theta}_1 + \dot{x}_1] - (1-\xi)I\dot{\theta}_1}{[\cos(\alpha-|\theta|)+\cos(\alpha+|\theta|)]R} \quad (26)$$

The above derivation is valid only if $|\int F_{xr}dt| \le \mu_s\left|\int F_{yr}dt\right| = \mu_s m(\dot{y}_1 - \dot{y}_2)$ and $S_\theta \int F_{xr}dt \le mS_\theta(\dot{x}_2 - \dot{x}_1)$. Note that $m(\dot{y}_1 - \dot{y}_2)$ is strictly positive, so the absolute sign is dropped.

Provided the friction is sufficient to prevent sliding (i.e. Eq. (23) holds true), if the computed impulse from Eq. (26) results in the violation of Eq. (21), then it is assumed that the impulses at the impact and rotation corners may be expressed as: $\int F_{xr}dt = m(\dot{x}_2 - \dot{x}_1)$ and $\int F_{xi}dt = 0$. With Eq. (18), ((26)), and ((30)), the postimpact velocities can be determined as:

$$\dot{\theta}_2 = \frac{\frac{1}{3}R\dot{\theta}_1 - \cos(\alpha-|\theta|)\dot{x}_1 + S_\theta \sin(\alpha-|\theta|)\dot{y}_1}{\frac{4}{3}R}; \dot{x}_2 = -R\cos(\alpha - |\theta|)\dot{\theta}_2;\ \dot{y}_2 = S_\theta R\sin(\alpha - |\theta|)\dot{\theta}_2 \quad (27)$$

In deriving Eq. (27), since $\int F_{xi}dt = 0$, Eq. (19) which involves the coefficient of restitution of the wall is assumed invalid. This, however, cannot ensure Eq. (22) is satisfied. Therefore, when the postimpact velocities derived from Eq. (27) violate Eq. (22), it is assumed that $\dot{x}_2 = R\cos(\alpha + |\theta|)\dot{\theta}_2$ to ensure compatibility. This leads to an indeterminate case since there are four conditions (i.e. Eq. (18), (20), (24) and $\dot{x}_2 = R\cos(\alpha + |\theta|)\dot{\theta}_2$) and only three unknowns (i.e. $\dot{x}_2$, $\dot{y}_2$, $\dot{\theta}_2$), making it impossible to get a solution that satisfies all the conditions. Consequently, it is proposed that by ignoring the momentum equilibrium the only compatible postimpact velocities are expressed in Eq. (28). Although the instantaneous postimpact velocities are zero, the block is deemed in rocking mode as it has finite rotation angle.

$$\dot{\theta}_2 = 0;\ \dot{x}_2 = 0;\ \dot{y}_2 = 0 \quad (28)$$

There is insufficient friction to prevent sliding during impact

If the computed impulse through Eq. (26) cannot meet the condition:$|\int F_{xr}dt| \le \mu_s\left|\int F_{yr}dt\right| = \mu_s m(\dot{y}_1 - \dot{y}_2)$, then Eq. (24) cannot be used since sliding happens during impact, but there is a new condition relating the horizontal and vertical impulse at the rotation corner:

$$\int F_{xr}dt = -\mu_k S_{\dot{x}_{r2}} \int F_{yr}dt = m\mu_k S_{\dot{x}_{r2}}(\dot{y}_2 - \dot{y}_1) \quad (29)$$

in which $S_{\dot{x}_{r2}} = S(\dot{x}_{r2})$.

Substituting Eq. (19), (20) and (29) into Eq. (18) gives the postimpact angular velocity:

$$\dot{\theta}_2 = \frac{\frac{1}{3}R\dot{\theta}_1 + \left[S_\theta \sin(\alpha-|\theta|) - \left(\cos(\alpha-|\theta|) + \cos(\alpha+|\theta|)\right)\mu_k S_{\dot{x}_{r2}}\right]\dot{y}_1 - e_w R\cos^2(\alpha+|\theta|)\dot{\theta}_1 + (e_w+1)\cos(\alpha+|\theta|)\dot{x}_1}{\frac{1}{3}R + \left[S_\theta \sin(a-|\theta|) - \left(\cos(\alpha-|\theta|) + \cos(\alpha+|\theta|)\right)\mu_k S_{\dot{x}_{r2}}\right]S_\theta R\sin(\alpha-|\theta|) + R\cos^2(\alpha+|\theta|)} \quad (30)$$

In Eq. (30), the only unknown is $S_{\dot{x}_{r2}}$. It can be assumed positive, which can then be verified by examining Eq. (14). The postimpact horizontal and vertical velocities can be found through Eq. (19) and (20) using the angular velocity from Eq. (30). They are not explicitly expressed here.

Similarly, it is also necessary to verify that the second physical constraint (i.e. Eq. (22)) of this problem is satisfied. If the impulse at the rotation corner $\int F_{xr}dt$, computed from Eq. (29), results in a violation of Eq. (22), the above-derived postimpact velocities from Eq. (30) are incorrect. Again, the impulses at the impact and rotation corner are assumed as: $\int F_{xr}dt = m(\dot{x}_2 - \dot{x}_1)$ and $\int F_{xi}dt = 0$. With Eq. (19), (20), and (29), the postimpact velocities are given as:

$$\dot{\theta}_2 = \frac{\frac{1}{3}R\dot{\theta}_1 - \mu_k S_{\dot{x}_{r2}}\cos(\alpha-|\theta|)\dot{y}_1 + S_\theta \sin(\alpha-|\theta|)\dot{y}_1}{\frac{1}{3}R + R\sin^2(\alpha-|\theta|) - \mu_k S_{\dot{x}_{r2}} S_\theta R\cos(\alpha-|\theta|)\sin(\alpha-|\theta|)};\ \dot{y}_2 = S_\theta R\sin(\alpha - |\theta|)\dot{\theta}_2; \dot{x}_2 = \mu_k S_{\dot{x}_{r2}}(\dot{y}_2 - \dot{y}_1) + \dot{x}_1 \quad (31)$$

Similarly, it is necessary to verify Eq. (22): if the postimpact velocities computed through Eq. (31) violate Eq. (22), then the momentum equilibrium is ignored, and the postimpact velocities are evaluated with Eq. (20), (29) and $\dot{x}_2 = R\cos(\alpha + |\theta|)\dot{\theta}_2$, which gives:

$$\dot{\theta}_2 = \frac{\mu_k S_{\dot{x}_{r2}}\dot{y}_1 - \dot{x}_1}{\mu_k S_{\dot{x}_{r2}} S_\theta R\sin(\alpha-|\theta|) - R\cos(\alpha+|\theta|)};\ \dot{y}_2 = S_\theta R\sin(\alpha - |\theta|)\dot{\theta}_2;\ \dot{x}_2 = R\cos(\alpha + |\theta|)\dot{\theta}_2 \quad (32)$$

The above formulation can be summarized by the flowchart shown in Fig. 3. A complete description for the other two cases can be found in [16].

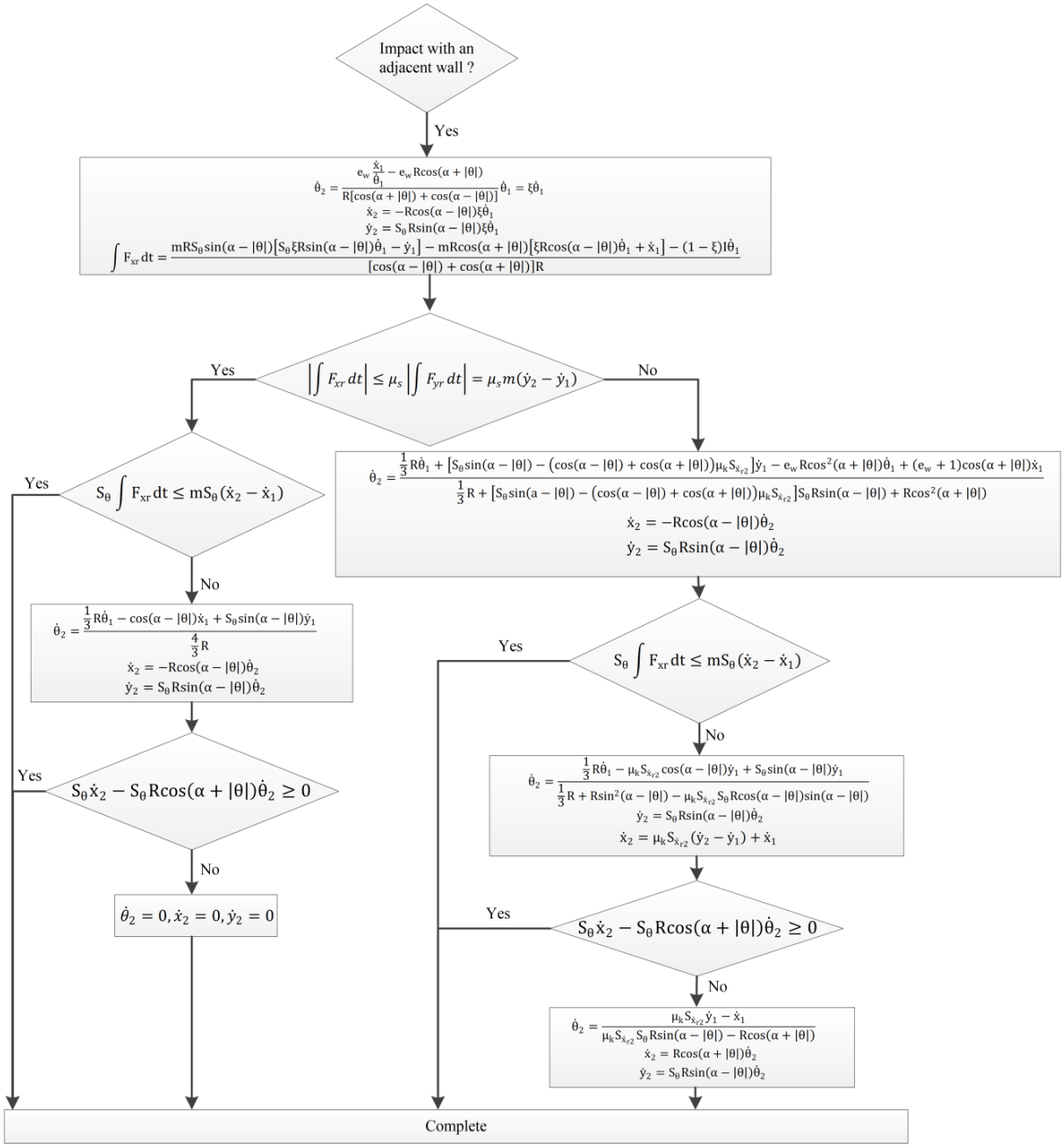

Fig. 3 Flowchart of approach to handle top corner impacting an adjacent wall

4. Numerical validation

This section presents the validation of the proposed numerical model. This is achieved by comparing the time history response with a general-purpose rigid body model in which impact and contact are modeled with a viscoelastic force model, as described in [17]. The rigid block model, with the governing equations of motion presented in Section 2, the treatment to handle impact with the ground in [11] and the approach to handle impact with adjacent wall in Section 3, is referred to in this paper as the *Event-Based Model* (EBM). The model developed in [17] uses rigid body dynamics and Kelvin-Voigt model for contact and impact with the base; as a result, the governing equation of motion is identical for all response modes. This model is referred to herein as the *Continuous Model* (CM). In this study the concentrated spring model is adopted for the CM; however, the damping component of the contact force is formulated using the following equations, as proposed in [18]:

$$c = 2\xi\sqrt{km};\ \xi = -\frac{\ln e}{\sqrt{\pi^2+(\ln e)^2}} \tag{33}$$

where k is the contact stiffness, c is the damping coefficient, ξ is the damping ratio, m is the mass of the block, and e is the coefficient of restitution of the wall or the ground.

Although it is not presented in [17], including an adjacent wall in the CM formulation is straightforward. This is achieved by tracking the horizontal coordinates of the four corners of the block. If penetration of any corner into an adjacent wall is detected during motion, then the contact force is initiated, and the contact force due to the rigid wall is formulated in the same way as the base.

For the remaining of this section, a rectangular rigid block with R = 1.605 m (i.e. frequency parameter p = 2.14 rad/s) and angle α = 0.25 rad is considered; or, equivalently, the block has dimensions of 2B = 0.794 m and 2H = 3.110 m. The friction coefficient of the base is selected as 0.3 (i.e. $\mu_k = \mu_s = 0.3$), which ensures that rocking motion will be initiated first. The coefficient of restitution between the base and the block is held constant at e_g = 0, which was shown in [11] to be equivalent to Housner's **Error! Reference source not found.** condition to ensure sustained rocking.

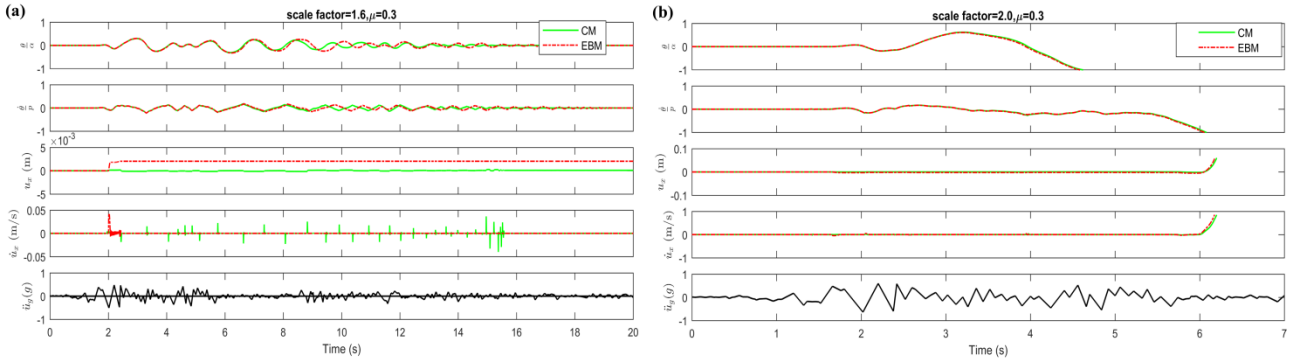

Fig. 4 Comparison of the responses of the block without an adjacent wall as computed using the CM and EBM. Excitation: 1940 Imperial Valley - El Centro ground motion (scaled)

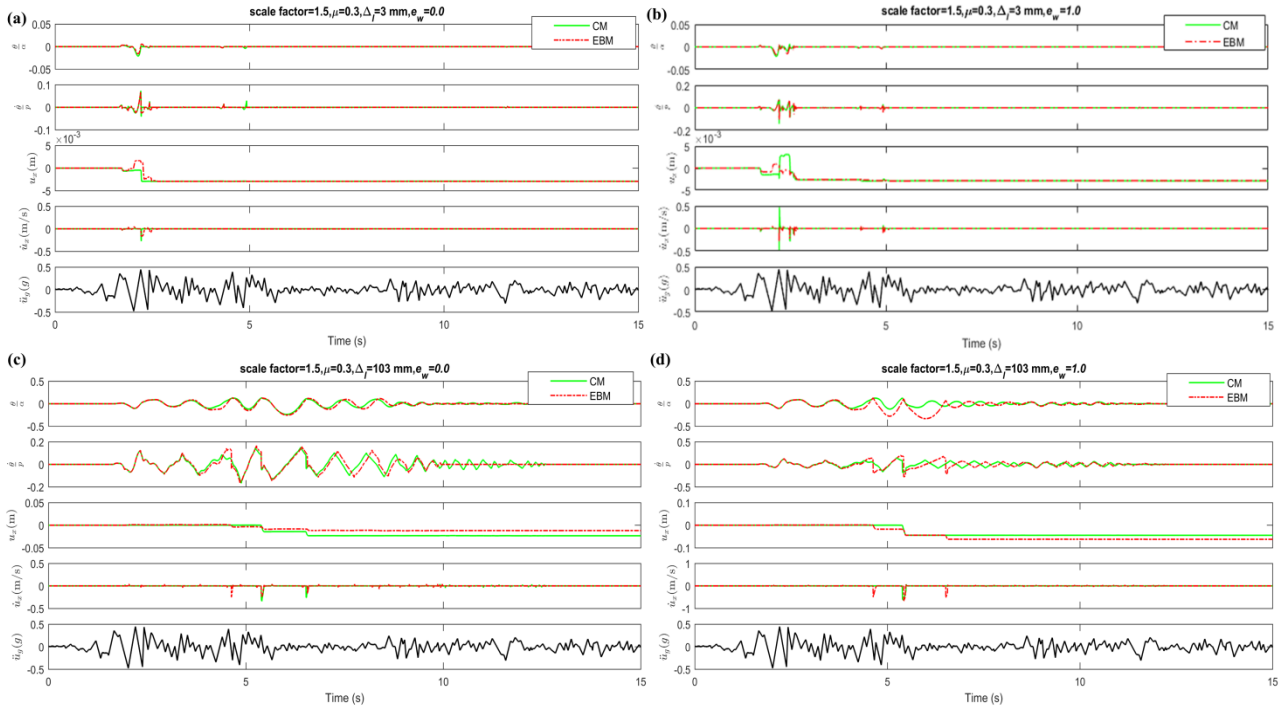

Fig. 5 Comparison of the responses of the block with an adjacent wall for a friction coefficient of 0.3

The time history comparisons of EBM and CM for both obstructed and unobstructed blocks are presented in Fig. 4 and Fig. 5. It is observed that in general these two models agree well, there are some minor differences regarding the horizontal velocities at the rotation corner. This difference is particularly notable left figure of Fig. 4 (i.e. Figure (a)). This may be attributed to the fact that CM uses a force-based method to handle the impact, which inevitably results in a short duration of free-flight of block, while the EBM assumes no free-flight can occur. For the brevity of this study, other combinations of block parameters are not included here for comparison purpose.

5. Effects of adjacent wall on the overturning of block

This section investigates effects of parameters associated with the adjacent wall on the overturning of the rigid block under pulse excitations. Overturning acceleration spectra are used to describe the behavior of rocking blocks under analytical pulse excitations. In this study, unsymmetric Ricker wavelets are used as input excitation to explore the toppling of the block with and without the presence of an adjacent wall. The ground acceleration corresponding to unsymmetric Ricker wavelet is defined by ([13], [14]):

$$\ddot{u}_g(t) = \frac{a_p}{1.38}\left(\frac{4\pi^2 t^2}{3T_p^2} - 3\right)\frac{2\pi t}{\sqrt{3}T_p} e^{-\frac{2\pi^2 t^2}{3T_p^2}} \tag{34}$$

where α_p is the amplitude of the Ricker pulse in units of g, and $T_p = 2\pi/\omega_p$ is the period. The block has the same dimensions as in Section 4 (i.e. p = 2.14 rad/s and α = 0.25 rad). Although both the EBM and CM are applicable, the former model is employed because construction of the overturning spectra requires thousands of analyses. The EBM is significantly more computationally efficient than the CM, and these two models provide similar predictions.

The horizontal axis of the overturning spectra is the normalized frequency ratio ω_p/p and the vertical axis is the normalized amplitude ratio $\alpha_p/g\tan\alpha$. The overturning spectra of the blocks with and without an adjacent wall are shown in Fig. 6 to Fig. 9 for comparison. In these figures the middle and right columns show the overturning spectra for different clear distances Δ and coefficients of restitution e_w values given the same friction coefficient and wall orientation, as labeled in each subplot title. The left column shows the corresponding overturning spectra of the unobstructed block for comparison purpose. In the middle and right columns, the blue region denotes a safe area, while the orange region represents toppling of the block. In the left column, the blue region denotes the block survives the pulses, yellow region denotes overturning in the clockwise direction, while overturning in the counterclockwise direction is shown in orange region.

When considering the presence of an adjacent wall, the following parameters may affect the shape of the overturning spectra: the coefficient of restitution of the wall e_w, the friction coefficient of the ground μ, the clear wall distance Δ, and the orientation of the wall. In this section, e_w is chosen as 0 or 1 to model purely elastic or plastic impact, μ is selected as 0.3 and 0.6, Δ is selected as 3, 53, and 103 mm. For each combination of these parameters, the adjacent wall can either be placed on the left side or the right side of the block. When the adjacent wall is on the left side, it can prevent the block from overturning in the counterclockwise direction. Similarly, the overturning mode in the clockwise direction is eliminated when the wall is placed on the right side. As the unobstructed block has two overturning modes, the orientation of the wall is expected to have a significant influence on the stability of the block.

Although including an adjacent wall further complicates the dynamic behavior of the rigid block subjected to unsymmetric Ricker wavelets, the general effects of different parameters can be evaluated by comparing the shapes of the overturning spectra. Keeping all other parameters the same, decreasing the friction coefficient μ, coefficient of restitution e_w, and clear distances Δ, can generally improve the stability of the blocks, as the safe areas in the overturning spectra expand. The wall orientation is the most important parameter being investigated. As the unobstructed block may overturn in counterclockwise or clockwise direction and it has a higher probability of overturning in the latter one, it is naturally presumed that placing the wall on the right side can improve the block's stability. However, numerical results presented in Fig. 8 and Fig. 9 suggest this intuitive conclusion may not be always true, depending on the combination of other parameters.

Generally, the effects of wall orientation are more evident when the friction coefficient is relatively small (i.e. μ = 0.3 in this study). In Fig. 8, it is observed that when the clear distance is only Δ_r = 3 mm and e_w = 0, the safe areas are greatly enhanced compared to those of the unobstructed counterpart. However, for the friction coefficient μ = 0.3 and clear distance of Δ_r = 103 mm, the presence of an adjacent right wall actually decreases the minimum acceleration required to overturn the block at high frequency (e.g. $\omega_p/p = 6$). When the friction coefficient is relatively large (i.e. μ = 0.6), the shape of the overturning spectra is largely affected only by the coefficient of restitution e_w. It is observed that when $\omega_p/p > 3$, there is almost no benefit in placing the wall on the right side for e_w = 0, while doing so results in a detrimental effect for e_w = 1.0. The situation where the adjacent wall is placed on the left side of the block is simpler. It can significantly decrease the safe area in the overturning spectra compared to the unobstructed counterpart in the high-frequency range; however, there are some stable regions in which overturning with one impact mode is eliminated when the wall is sufficiently close to the block (e.g. ω_p/p ranging from 2 to 3 with clear distance Δ_l =3 mm and e_w = 0.0).

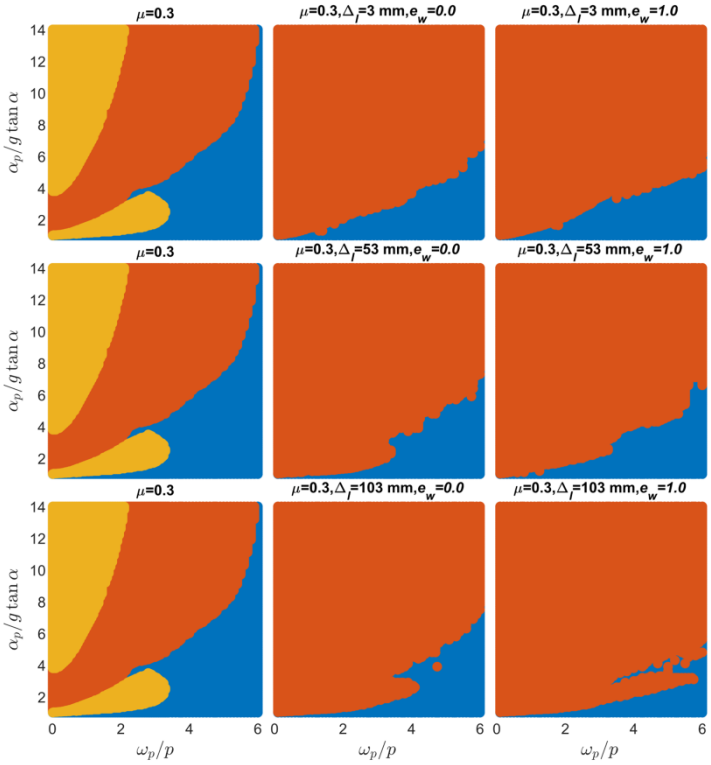

Fig. 6 Overturning spectra with an adjacent left wall when friction coefficient μ = 0.3

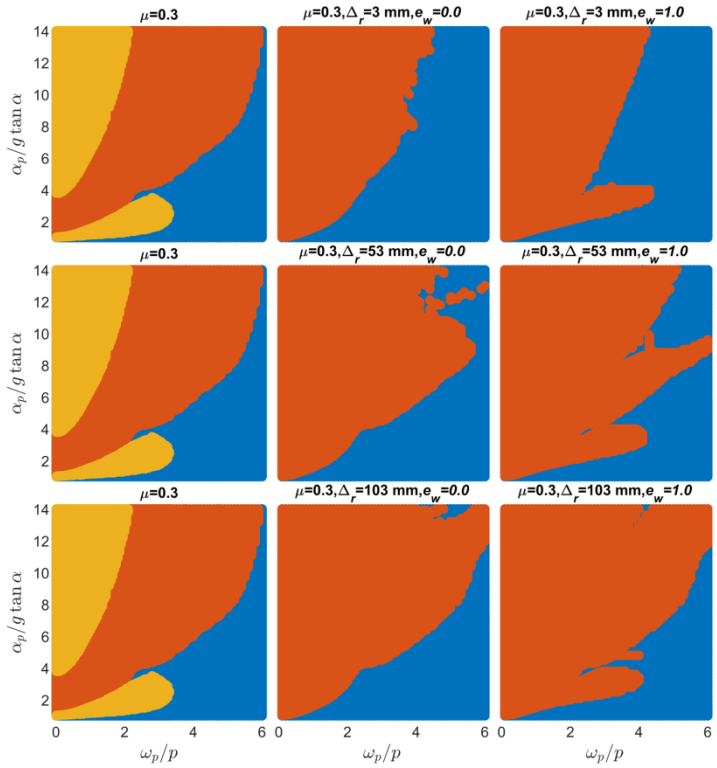

Fig. 7 Overturning spectra with an adjacent left wall when friction coefficient μ = 0.6

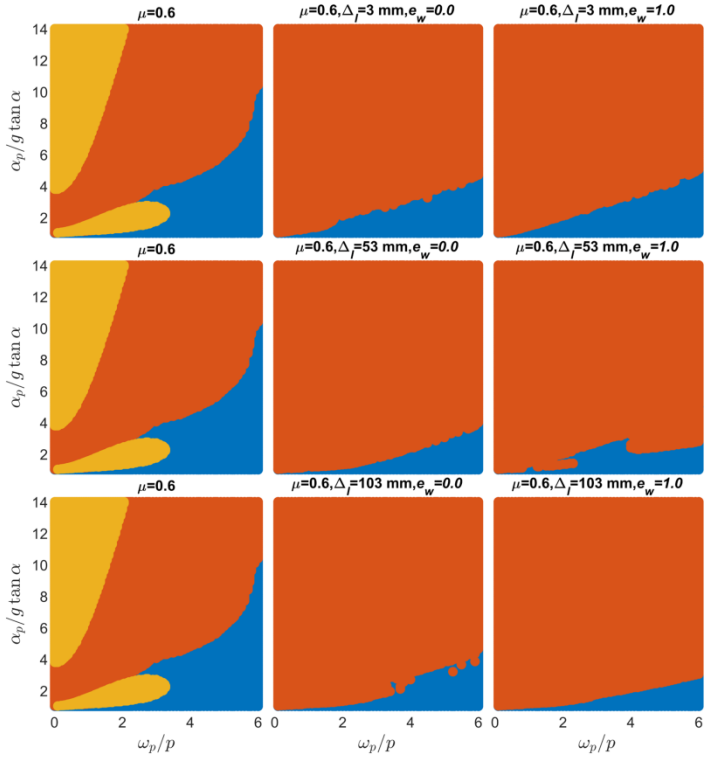

Fig. 8 Overturning spectra with an adjacent right wall when friction coefficient μ = 0.3

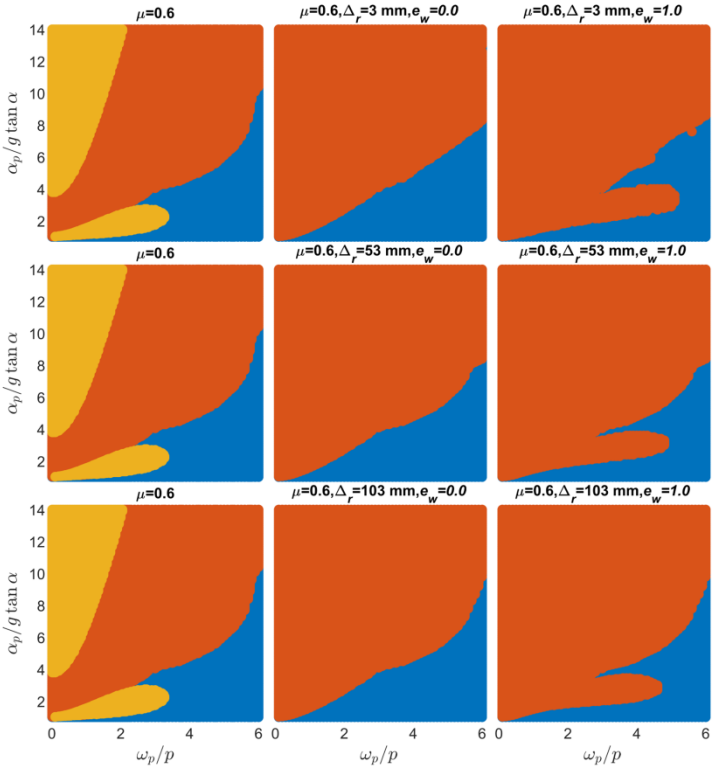

Fig. 9 Overturning spectra with an adjacent right wall when friction coefficient μ = 0.6

6. Conclusions

This paper investigates the dynamics of a two-dimensional sliding-rocking block considering impact with an adjacent wall. Based on the classical impulse and momentum theory and the assumption that free-flight mode is excluded, the first phase of this paper describes an approach to handle the planar block impacts with an adjacent wall. The time history responses of the Event Based Model developed in this paper are compared with an existing Continuous Model under El Centro ground motion. These comparisons consider the presence and absence of the adjacent wall, and results indicate the Event Base Model can provide reasonable accuracy in both cases.

The second phase of this paper investigates the effects of different parameters on the overturning spectra of rigid blocks under unsymmetric Ricker wavelets. The Event Based Model is used for this investigation due to its high computational efficiency.

For the overturning spectra, when considering the presence of an adjacent wall, the problem becomes very complex due to its highly nonlinear nature and large combinations of parameters. In general, it is concluded that decreasing the coefficient of the restitution of the wall, decreasing the friction coefficient and clear distance have beneficial effects on stabilizing the block. The orientation of wall has a dominant effect on the shape of overturning spectra. Placing the wall in a direction that an unobstructed block has less probability to overturn (i.e. left side in this study) has detrimental effect on the stability. However, placing the wall in the opposite direction does not necessarily guarantee the beneficial effect. Such beneficial effect directly depends on the combination of other parameters such as friction coefficient and clear distance. The model developed in this paper will facilitate in the development of useful fragility curves for non-structural components in real buildings.

7. References

[1] Housner GW. The behavior of inverted pendulum structures during earthquakes. *Bulletin of the Seismological Society of America*, 1963, 53(2): 403-417.

[2] Shenton HW. Criteria for initiation of slide, rock, and slide-rock rigid-body modes. *Journal of Engineering Mechanics*, 1996, 122(7): 690-693.

[3] Konstantinidis D and Nikfar F. Seismic Response of Sliding Equipment in Base Isolated Buildings Subjected to Broad-Band Ground Motions, *Earthquake Engineering and Structural Dynamics*, 2015, 44(6): 865-887.
[4] Nikfar F and Konstantinidis D. Peak sliding demands on unanchored equipment and contents in base-isolated buildings under pulse excitation. *Journal of Structural Engineering*, 2017, 143(9):04017086.
[5] Konstantinidis D, and Makris N. Experimental and analytical studies on the response of freestanding laboratory equipment to earthquake shaking. *Earthquake Engineering and Structural Dynamics*, 2009, 38(6), 827–848.
[6] Zhang J and Makris N. Rocking response of free-standing blocks under cycloidal pulses. *Journal of Engineering Mechanics*, 2001, 127(5): 473-483.
[7] Makris N and Vassiliou MF. Sizing the slenderness of free-standing rocking columns to withstand earthquake shaking. *Archive of Applied Mechanics*, 2012, 82(10-11), 1497-1511.
[8] Mochizuki T and Kobayashi K. A study on acceleration of earthquake motion deduced from the movement of column: an analysis on the movement of column. *Transactions of the Architectural Institute of Japan*, 1976, 248, 63-70. (in Japanese)
[9] Ishiyama Y. Motions of rigid bodies and criteria for overturning by earthquake excitations. *Earthquake Engineering and Structural Dynamics*, 1982, 10: 635-650.
[10] Taniguchi T. Non-linear response analyses of rectangular rigid bodies subjected to horizontal and vertical ground motion. *Earthquake Engineering and Structural Dynamics*, 2002, 31: 1481-1500.
[11] Shenton HW and Jones NP. Base excitation of rigid bodies. I: formulation. *Journal of Engineering Mechanics*, 1991, 117(10): 2286- 2306.
[12] Filiatrault A, Kuan S and Tremblay R. Shake table testing of bookcase-partition wall systems. *Canadian Journal of Civil Engineering*, 2004, 31: 664-676.
[13] Ricker N. Wavelet functions and their polynomials. *Geophysics*, 1944, 9:314-323.
[14] Ricker N. Further developments in the wavelet theory of seismogram structure. *Bulletin of the Seismological Society of America*, 1943, 33:197-228.
[15] Konstantinidis D and Makris N. Experimental and analytical studies on the seismic response of freestanding and anchored laboratory equipment. PEER Report 2005, Pacific Earthquake Engineering Research Center, University of California at Berkeley.\
[16] Bao Y and Konstantinidis D. Dynamics of a sliding-rocking block considering impact with an adjacent wall. *Earthquake Engineering and Structural Dynamics*. DOI:10.1002/eqe.3250. (In Press)
[17] Chatzis MN and Smyth AW. Robust modeling of the rocking problem. *Journal of Engineering Mechanics*, 2012, 138(3): 247- 262.
[18] Anagnostopoulos SA. Equivalent viscous damping for modeling inelastic impacts in earthquake pounding problems. *Earthquake Engineering and Structural Dynamics*, 2004, 33: 897- 902.

